Original Article

High-temperature reactions and phase evolution in precursor-derived ZrB_2/Si-C-N composites

Ingo Jürgen Markel*, Jürgen Glaser, Martin Steinbrück, Hans Jürgen Seifert

Institute for Applied Materials-Applied Materials Physics, Karlsruhe Institute of Technology, Germany

ARTICLE INFO

Keywords:
CALPHAD
Polysilazane
CMC
High-temperature reactions
Thermodynamics

ABSTRACT

A ZrB_2/Si-C-N composite was prepared by pyrolysis of a ZrB_2-powder containing polysilazane (Ceraset® PSZ 20) at maximum temperatures of 1200 °C, 1300 °C, 1400 °C, and 1500 °C in flowing pure Ar- and Ar/N_2-atmospheres. In combination with thermogravimetry, mass spectrometry, XRD and SEM the chemical compatibility of the ZrB_2-additive, limiting the high-temperature application, was investigated. Additionally, phase stabilities and intrinsic high-temperature reactions between the ZrB_2-additive and the Si-C-N ceramic components (Si_3N_4, SiC and C) were modeled using the CALPHAD method. The first reaction was found to occur 113 °C above the Si-C-N-internal decomposition reaction. Thermodynamic conditions for the formation as well as the avoidance of ZrC_xN_y were derived with respect to temperature and atmosphere (p_{N2}). Out of this, a formation mechanism of ZrC_xN_y was proposed consisting of a solid-gas reaction during pyrolysis of the ZrB_2/Si-C-N composite forming ZrN followed by the uptake of graphite from the Si-C-N ceramic.

1. Introduction

Due to their excellent high temperature stability, low density and thermal shock resistance, SiC based ceramic matrix composites (CMCs) are promising structural materials for high temperature applications in aerospace re entry vehicles and hot sections of turbines for aviation and electrical power generation, respectively. SiC fiber reinforced SiCN matrix composites ($SiC_f/SiCN_m$) can be manufactured via the polymer infiltration and pyrolysis (PIP) process. A fiber preform is infiltrated with a liquid preceramic polymer (polysilazane) which is subsequently transformed into a solid, amorphous Si C N ceramic by thermal curing and pyrolysis. The composition of carbon rich Si C N ceramics with a Si/C ration of < 1, such as PSZ 20, is within the three phase field SiC + Si_3N_4 + C if crystallization would occur [1 3]. The application temperature is thereby limited by the internal phase reactions:

At 1484 °C: $Si_3N_4 + 3C = 3SiC + 2N_2\uparrow$

And at 1841 °C: $Si_3N_4 = 3Si_l + 2N_2\uparrow$

By addition of fillers, improved properties of the material can be achieved. It was also demonstrated that reactive active fillers, which undergo a volume expansion, can be used to improve porosity and di mensional change of the ceramic matrix [4 6]. She et al. [7] showed that the volume increase due to the nitriding reaction of ZrB_2 to form ZrN is capable to heal surface defects and reduce the amount of surface connected pores. Therefore, a targeted conditioning of ZrB_2/Si C N composites in N_2 after manufacturing could be conducted to promote self healing. Furthermore a protective effect of boron containing com ponents on the oxidation behavior of SiC based ceramics by formation of a boro silicate glass (eutectic temperature 440 °C [8]) was demon strated for BN fiber coatings [9], bulk ZrB_2 SiC (and HfB_2 SiC) ultra high temperature ceramics (UHTC) [10,11] and boron containing Si B C N precursor ceramics [12]. Besides these polyborosilazanes, were boron is chemically bonded in the precursor polymer chain [13,14], the use of a ZrB_2 filler in Si C N polymer precursors could be a cost effec tive way to introduce boron into the ceramic matrix. While most of the work on ZrB_2 SiC focuses on the synthesis [15] and oxidation resistance [16,17] of these materials, only few studies were carried out on the high temperature stability of ZrB_2/Si C N composites [18].

The focus of this work was to investigate the fundamental hetero geneous reactions in the ZrB_2/Si C N basis material, however without the influence of an oxidizing atmosphere. Therefore, interactions of ZrB_2 with thermodynamic stable phases in the PSZ 20 derived Si C N matrix were modelled with a specifically developed CALPHAD dataset. Out of this, the high temperature stability of a ZrB_2/Si C N composite was derived. Furthermore, the formation mechanism of ZrC_xN_y was discussed on the basis of thermodynamic equilibrium calculations.

* Corresponding author.
E-mail addresses: ingo.markel@kit.edu, ingojm@t-online.de (I.J. Markel).

2. Experimental

The ceramic matrix of the ZrB_2/Si C N composite was prepared from the pre ceramic polymer Ceraset® Polysilazane 20 (PSZ 20) by Clariant SE, Germany. ZrB_2 powder from H.C. Starck (97% purity, average particle size 3.2 µm) was added and homogenized by thorough stirring. The obtained slurry with a ZrB_2 content of 12 23 wt.% was pyrolyzed in flowing pure Ar (Ar 6.0, 99.9999% purity) or Ar/N_2 at mospheres (N_2 6.0, 99.9999% purity, p_{N2} = 0.5 bar) using a Netzsch STA 449 F3 Jupiter equipped with alumina crucibles. To ensure proper outgassing and crosslinking of the polymer, samples were gradually heated to 300 °C in several steps. Samples were then heated with 5 °C/min from 300 °C to the final pyrolysis temperature of 1200 °C, 1300 °C, 1400 °C or 1500 °C, held for 5 h at these temperatures and cooled down to room temperature with 20 °C/min.

Isothermal nitriding kinetics of pure ZrB_2 powders were in vestigated in flowing Ar/N_2 (p_{N2} = 0.5 bar). In order to avoid unin tended oxidation of the samples by oxygen impurities the STA was equipped with a Zr oxygen getter. Resulting oxygen partial pressures were below $2{\cdot}10^{-13}$ ppm. The mass conversion degree α was calculated using Eq. (3):

$$\alpha = \frac{w_i - w_0}{w_f - w_0} \tag{3}$$

with w_i, w_0 and w_f denoting the intermediate, initial and final sample mass for complete reaction.

The Johnson Mehl Avrami Kolmogorow (JMAK) Eq. (4) [19 21]:

$$\alpha(t) = 1 - exp(-(k{\bullet}t)^n) \tag{4}$$

was used to determine the reaction rate constant k and the Avrami exponent n of the nitriding reaction.

The ZrB_2/Si C N composite, resulting from this procedure, was in vestigated by SEM (Philips XL 30 S FEG). Phase analysis was carried out using a Seifert PAD II powder diffractometer in Bragg Brentano geo metry with monochromatic Cu Kα radiation (λ = 0.15418 nm). To this end, samples were ground in an agate mortar.

3. Thermodynamic modelling

The CALPHAD (CALculation of PHAse Diagram) method [22] was used to compute phase equilibria in the multicomponent Zr Si B C N system. Thermodynamic data for the pure elements were taken from the SGTE Unary database PURE v5.1 [23]. Binary systems Si C [24], Si N [8], Si B [8], B C [8], B N [8], Zr Si [25], Zr N [26], Zr B [25], and Zr C [27] were accepted from literature. The ternary systems B C N, B C Si and B N Si were adopted from Kasper [8]. Additionally, the ternary systems Zr Si C [28] and Zr B C [29] were considered. In order to ob tain compatibility of the thermodynamic liquid phase description, using by different models in literature, the liquid phase was modeled by a partially ionic sublattice model. Therefore the interaction parameters of the liquid phase were reoptimized for the binary systems Zr N and Zr C (see Table 1). The resulting binary phase diagrams are depicted in Fig. 1. Gas species were added from the SGTE substance database SSUB v4.1 [23]. Since there are no ternary or higher order compounds, it was possible to extrapolate from these unary, binary and ternary phase diagram data to the quinary Zr Si B C N system using the CALPHAD method. The obtained dataset was used to perform equilibrium calcu lations and compute property diagrams employing the Thermo Calc [30] software.

Table 1
Reoptimized interaction parameters of the liquid phase for the binary systems Zr-C and Zr-N. The thermodynamic coefficients for the solid phase descriptions of these systems can be found in literature [26,27].

Ionic Liquid $(B^{+3},Si^{+4},Zr^{+4})_P(C,N,SiN_{4/3},Va)_Q$	
L_0(Ionic Liquid, Zr^{+4} : C, Va)	= 310,825.555 + 17.8033498·T
L_1(Ionic Liquid, Zr^{+4} : C, Va)	= +39,539.7481
L_2(Ionic Liquid, Zr^{+4} : C, Va)	= +50000
L_0(Ionic Liquid, Zr^{+4} : N, Va)	= 249,605.669 - 65.2089004·T
L_1(Ionic Liquid, Zr^{+4} : N, Va)	= +152,559.417 - 48.3959946·T
298.15 K 6000 K	

Zirconium carbide and nitride are both crystallizing in the cubic NaCl type structure with the space group $Fm\bar{3}m$ (No. 225). Both are sub stoichiometric (ZrC_{1-x} and ZrN_{1-x}) with $0.64 < x < 0.5$ and $0.38 < x < 0.5$, respectively. According to that, ZrC_{1-x} and ZrN_{1-x} are described by a face centered cubic model with two sublattices in CALPHAD [27,26]. The first sublattice is occupied by zirconium while the second sublattice can contain the elements carbon and nitrogen as well as vacancies (Va) which are accommodating the sub stoichiometry of the phases or boron as solution element. The site occupancy of the second sublattice thereby accounts for the formation of solid solutions, for instance C in ZrN_{1-x}. ZrB_2 has a hexagonal crystal structure with the space group P6/mmm (No. 191) and is modelled as a stoichiometric phase according to [25].

Calculations were performed as a closed system with a constant substance amount of n = 1 mol and a self developing gas volume at a constant gas pressure of $p = 10^5$ Pa. Argon was used as inert gas to generate a stable gas phase at any temperature during calculation. For calculation of the phase fraction diagrams, a composition of 49 at.% ZrB_2, 1 at.% Ar and 50 at.% of C, SiC or Si_3N_4 was assumed as starting composition.

4. Results

4.1. Thermodynamic calculations

Thermodynamic equilibrium calculations were performed to vali date the compatibility of the ZrB_2 additive with the Si C N ceramic components C, SiC and Si_3N_4, assuming crystallization, and to clarify if reactions take place which lower the maximum application temperature of the Si C N ceramic. Phase fraction diagrams for reactions of me chanical powder mixtures of ZrB_2 + C and ZrB_2 + SiC as a function of the temperature are shown in Fig. 2. The phase fractions of ZrB_2 and C as well as ZrB_2 and SiC are both constant up to melt formation at tem peratures above 2250 °C. This result is indicating that ZrB_2 is chemi cally inert with the Si C N components C as well as SiC.

For the mechanical powder mixture $ZrB_2 + Si_3N_4$ several reactions are evident from the phase fraction diagram and the associated gas phase composition in Fig. 3:

$$1597\,°C:\ ZrB_2 + Si_3N_4 = ZrN + 2BN + L(\underline{Si}, Zr, B, N) \tag{5}$$

$$1912\,°C:\ ZrN + 2BN = ZrB_2 + 3/2N_2\uparrow \tag{6}$$

The first reaction to occur is between ZrB_2 and Si_3N_4 at 1597 °C. ZrN and BN are formed and a melt, consisting mainly of Si and minor amounts of Zr, B and N (see Fig. 3c). At 1912 °C ZrN and BN are reacting under formation of ZrB_2 and N_2, which is released to the gas phase (see Fig. 3b). In addition, under excess of Si_3N_4 compared to ZrB_2, the re maining Si_3N_4 is thermally decomposed to liquid Si and N_2 at 1818 °C. Due to the chemical composition of the melt, which is formed in re action (5), the decomposition temperature is 23 °C lower compared to Si_3N_4 alone.

The Zr B N system

The stability of ZrB_2 strongly depends on the activity of nitrogen in the atmosphere, denoted here as the nitrogen partial pressure (p_{N2}) of the atmosphere and can be derived from the p_{N2} T diagram in Fig. 4. As the formation of other gas species is negligible, the partial p_{N2} is equal to the total pressure. Solid phases in equilibrium, with N_2 as the gas phase, are indicated. The line corresponds to the univariant three phase equilibrium ZrB_2 + ZrN + BN whereas the areas below and above

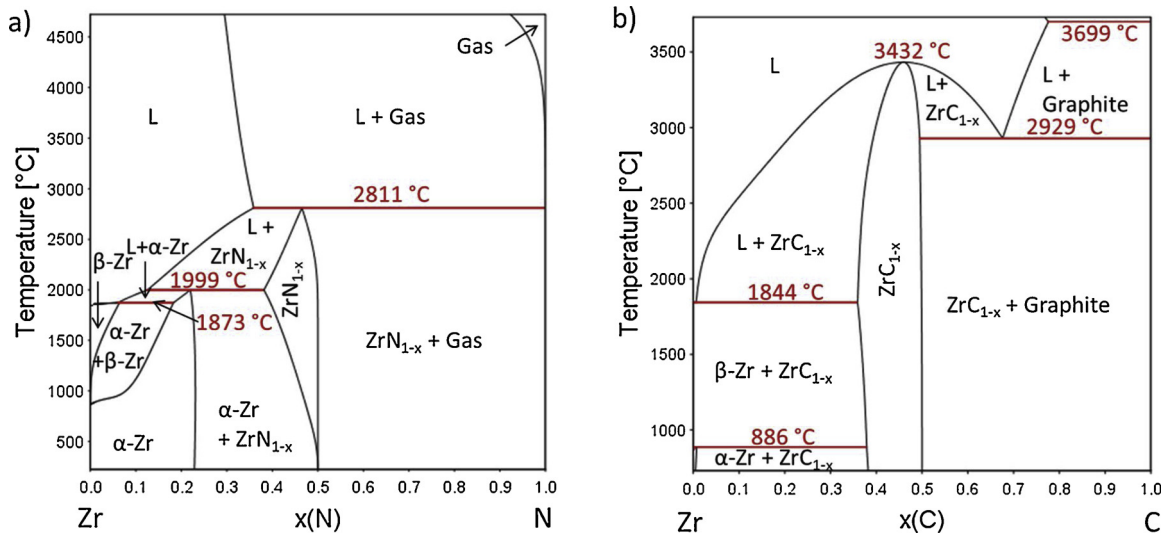

Fig. 1. Calculated phase diagrams of the binary systems a) Zr-N and b) Zr-C.

correspond to the divariant single phase equilibrium ZrB_2 and the two phase equilibrium ZrN + BN, respectively. Thus, ZrB_2 is stable at high temperature and low p_{N2}. Upon crossing the line, the nitriding reaction $ZrB_2 + 3/2N_2 = ZrN + 2BN$ takes place. In pure nitrogen at ambient pressure (p_{N2} = 1 bar), the nitriding reaction takes place above 1918 °C. Lower nitrogen partial pressures result in an extension of the ZrB_2 stability field to lower temperatures of 1842 °C and 1686 °C at p_{N2} = 0.5 bar and 0.1 bar, respectively.

The Zr C N system

To understand the interaction of ZrN with graphite as a component of the PSZ 20 derived ceramics, the phase fraction diagram, site occupancies of the resulting ZrC_xN_y phase and the composition of the associated gas phase were calculated.

The phase fraction diagram showing the reaction of ZrN with graphite as a function of the carbon activity at 1200 °C, 1300 °C, 1400 °C, and 1500 °C is depicted in Fig. 5. With increasing carbon activity, carbon is occupying the second sublattice of the ZrN phase forming ZrC_xN_y. As a result, the site fraction of N is decreasing (see Fig. 5b) and N_2 is released to the atmosphere (see Fig. 5c). Therefore the relative phase fraction of ZrC_xN_y is decreasing while the relative amount of the gas phase is increasing (see Fig. 5a). The solubility of C in ZrC_xN_y is thereby increasing with temperature.

The phase fraction diagram of ZrC_xN_y in thermodynamic equilibrium with graphite is shown in Fig. 6a. Starting from approximately 900 °C, the phase fraction of graphite is decreasing while the amount of gas is increasing. The site occupancy of the second sublattice of ZrC_xN_y, shown in Fig. 6b, is thereby shifted from N rich at low temperatures to C rich at high temperatures with a point of inversion at 1699 °C. Vacancies are formed at the highest temperatures. Fig. 6c reveals the release of N_2 into the gas phase during this process.

4.2. Experimental investigations

The thermogravimetric analysis of the preparation process starting from ZrB_2 containing PSZ 20 slurry to the ZrB_2/Si C N composite is shown in Fig. 7. For better comparability, the mass change of the ZrB_2 containing samples was normalized to their PSZ 20 content. Results for pure PSZ 20 [3] are shown for comparison. During the first stage, the liquid polysilazane PSZ 20 is crosslinked by stepwise heating to 300 °C. In this process the evaporation of oligomers as well as the formation of bonds between different polymer chains under release of gaseous, hydrogen containing molecules (H_2, CH_4,…) are resulting in the observed mass loss. In the second stage, the actual pyrolysis process is taking place: the crosslinked PSZ 20 is transformed into the solid Si C N ceramic. The mass loss observed during pyrolysis accounts for the release of hydrogen, which is an intrinsic part of the polymer chain in form of hydrogen containing gas species. In stage 3 a holding time of 5 h at final temperatures of 1200 °C, 1300 °C, 1400 °C and 1500 °C was applied to ensure a complete transformation and to allow reactions within the Si C N matrix or with the ZrB_2 additive to take place.

Samples which were heat treated up to 1200 °C and 1300 °C in Ar show a constant mass above approx. 900 °C. An additional mass loss is

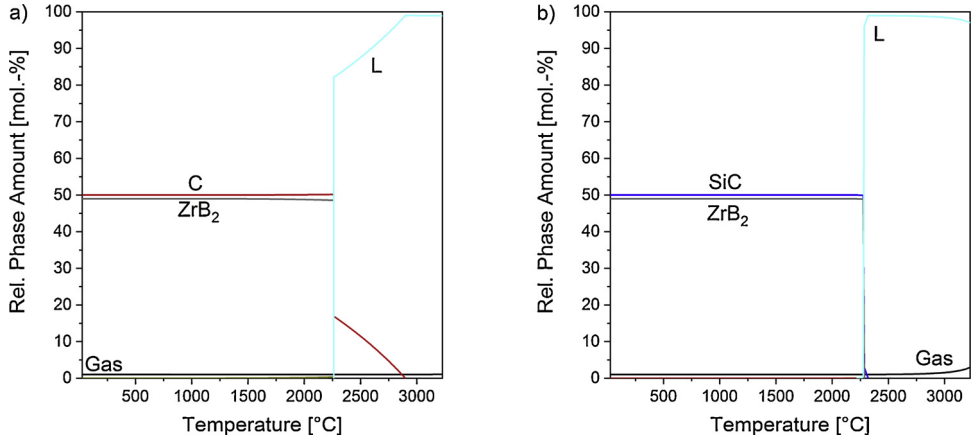

Fig. 2. Temperature dependence of the phase fractions of the initial couples a) ZrB_2 + C and b) ZrB_2 + SiC.

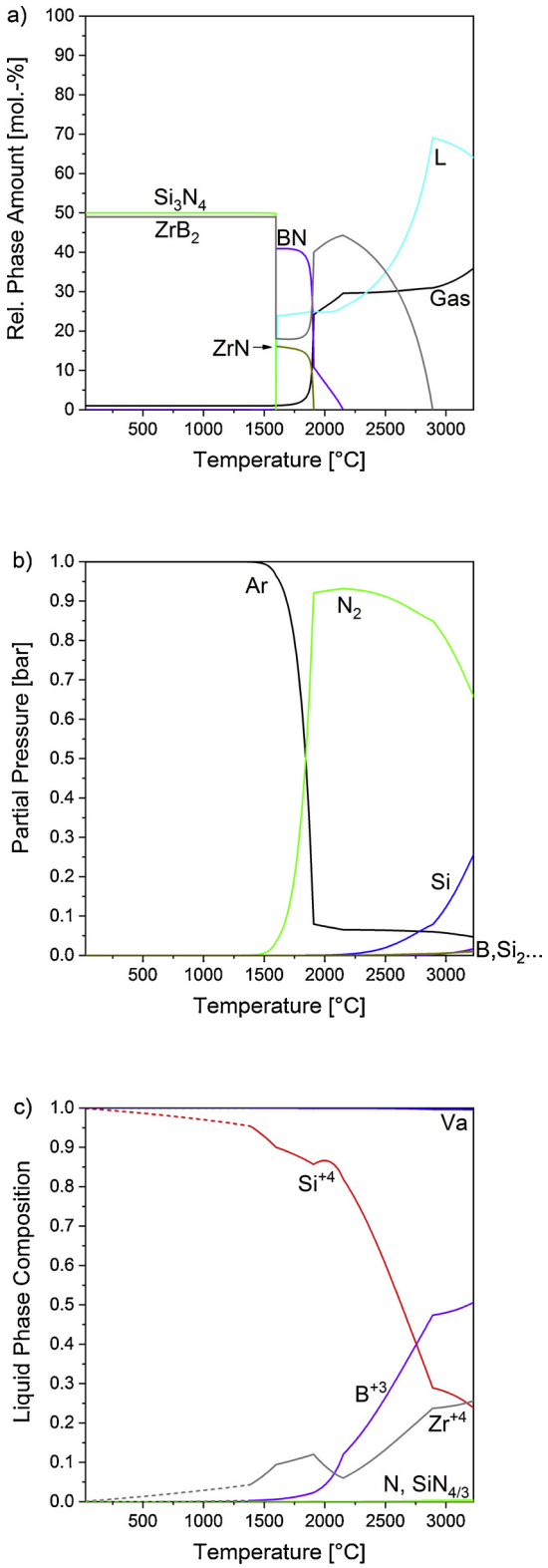

Fig. 3. Temperature dependence of the a) phase fractions and b) composition of the associated gas phase and c) composition of the liquid phase for the initial couple $ZrB_2 + Si_3N_4$.

observed for samples which were heat treated up to 1400 and 1500 °C. Experiments in Ar/N_2 atmosphere resulted in a considerably smaller mass loss at 1400 °C and 1500 °C compared to pure Ar. ZrB_2 containing samples show in addition a higher scattering due to spallation of sample parts.

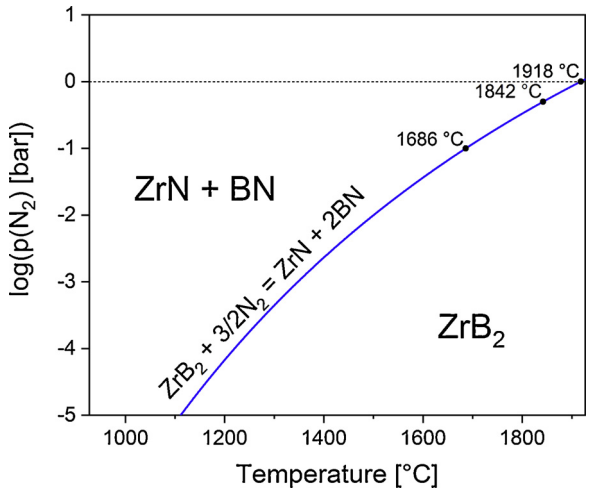

Fig. 4. Phase equilibria in the Zr-B-N system as a function of p_{N2} and temperature.

The ZrB_2 particles are homogeneously distributed in the resulting ZrB_2/Si C N composite as depicted in Fig. 8. Cracks are resulting from shrinkage during pyrolysis of the preceramic polymer PSZ 20. The Si C N matrix is very homogeneous for samples heat treated up to 1400 °C in Ar/N_2 atmosphere and at 1200 °C and 1300 °C in pure Ar. However, heat treatment at 1500 °C, and partly at 1400 °C in Ar, results in a de gradation reaction and a porous appearance of the Si C N matrix.

Fig. 9 shows XRD patterns of the obtained ZrB_2/Si C N ceramics. Reflections of ZrB_2 are present at all temperatures and in both atmo spheres. Crystallization of β SiC from the Si C N matrix is observed after pyrolysis and heat treatment at 1400 °C and 1500 °C in Ar. At lower temperatures in Ar and at all temperatures in Ar/N_2 atmosphere the Si C N matrix is X ray amorphous. ZrC_xN_y formation is observed after preparation at 1300 °C, 1400 °C and 1500 °C in Ar/N_2. In pure Ar atmosphere ZrC_xN_y formation primarily occurs at 1400 °C. At all other temperatures, especially 1500 °C ZrC_xN_y formation is much less pro nounced compared to pyrolysis in Ar/N_2. The peak positions of ZrC and ZrN are indicated for comparison. Additionally, silicon is formed at 1500 °C in pure Ar and α Si_3N_4 in Ar/N_2 at 1300 °C, 1400 °C and 1500 °C. The crystallization of PSZ 20, depending on the nitrogen partial pressure, was investigated in an earlier work [3].

XRD patterns of ZrB_2 powder isothermally annealed at 1200 °C, 1300 °C, 1400 °C and 1500 °C in an Ar/N_2 atmosphere are shown in Fig. 10. Besides the reflections of the ZrB_2 powder, the evolution of ZrN reflections is observed with increasing annealing temperature. To a very small extent, cubic ZrO_2 is present independent from temperature. Unindexed tiny reflections in Figs. 9 and 10 correspond to K_β reflections of the high intensity ZrB_2 peaks.

The mass conversion degree during isothermal nitriding of pure ZrB_2 powders is shown in Fig. 11a. Isothermal nitriding at 1200 °C, 1300 °C, and 1400 °C results in linear nitriding kinetics. Parameters are summarized in Table 2. An apparent activation energy of the nitriding process of 154 kJ/mol is obtained from the Arrhenius plot of the linear reaction constant k_l (Fig. 11b). However, nitriding at 1500 °C follows a more complex process and was therefore not considered for kinetic evaluation.

5. Discussion

Modeling of the individual high temperature reactions between the ZrB_2 additive and the Si C N matrix components (ZrB_2 + C, ZrB_2 + SiC, $ZrB_2 + Si_3N_4$) revealed the primary occurrence of interactions for $ZrB_2 + Si_3N_4$ at 1597 °C. The reaction $ZrB_2 + Si_3N_4 = ZrN + 2BN$ + L oc curs 113 °C above the internal matrix reaction (1). Therefore, the re levant application temperature of this Si C N matrix system is not

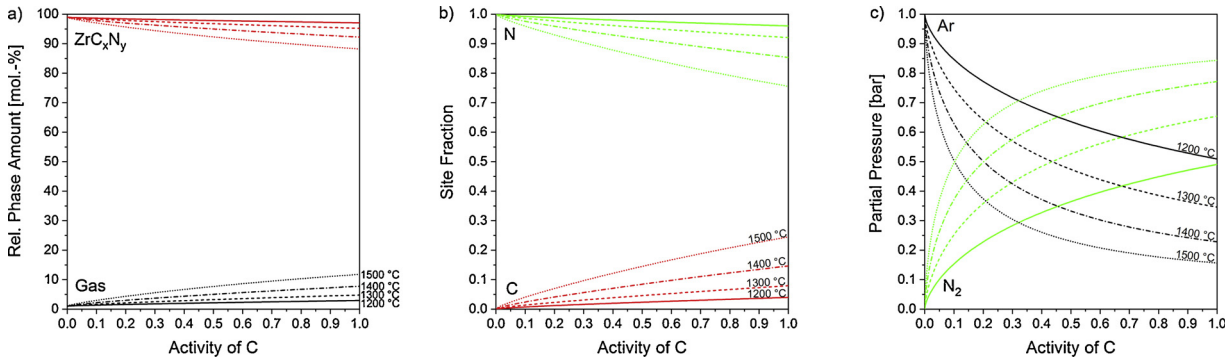

Fig. 5. Calculated a) phase fraction b) site occupancy and c) gas composition for ZrC_xN_y as a function of the carbon activity at 1200 °C, 1300 °C, 1400 °C and 1500 °C.

reduced. Guo et al. [31,32] also observe the reaction of ZrB_2 and Si_3N_4 in Ar only from 1600 °C. $ZrSi_2$ which was observed in that study might by formed by solidification of the Si and Zr containing melt. The matrix components SiC and C do not show interactions with the ZrB_2 additive up to melt formation above 2286 °C and 2262 °C, respectively. This is in good accordance with the work by Kaufman [33] who calculated eutectic temperatures of 2207 °C and 2390 °C 2427 °C for ZrB_2 SiC and ZrB_2 C, respectively. In addition, Nasiri et al. [34] found no interaction in ZrB_2 SiC C_{sf} composites up to the highest experimentally investigated temperature of 2150 °C. Calculating with the thermodynamic stable crystalline components of the amorphous Si C N matrix is valid, as detailed earlier studies have demonstrated the presence of structural units (CSi_4, SiN_xC_y (x = 2.3; x + y = 4), SiN_4 and sp^2 hybridized carbon) of the thermodynamically stable crystalline phases SiC, Si_3N_4 and C already within the amorphous structure of Si C N ceramics [35 38].

The formation mechanism of the ZrC_xN_y solid solution from the ZrB_2/Si C N composite is discussed below. A primary reaction of the ZrB_2 additive with free graphite from the Si C N matrix can be excluded from the CALPHAD modelling and was also excluded experimentally by Brewer et al. [39]. It can also be excluded that ZrB_2 is reacting with Si_3N_4 from the Si C N matrix as this reaction is only expected at higher temperatures. Instead, more pronounced ZrC_xN_y formation in Ar/N_2 compared to pure Ar (Fig. 9) and ZrN formation during isothermal nitriding experiments of pure ZrB_2 indicate an initial solid gas reaction of ZrB_2 and N_2.

CALPHAD modelling of the phase stability fields (Fig. 4) showed that ZrB_2 is stable at high temperatures and low p_{N2} and forms ZrN at "low" temperatures and high p_{N2}, respectively. With decreasing p_{N2} the stability range of ZrB_2 is extended to lower temperatures. This accounts for the presence of ZrC_xN_y formation in Ar/N_2 atmosphere. Pyrolysis in Ar atmosphere (see Fig. 9a) results in a significant reduction of ZrC_xN_y formation, especially at the highest temperature of 1500 °C. The only exception is at 1400 °C in Ar where ZrC_xN_y is also formed. Combined TG MS investigations of PSZ 20 pyrolysis and high temperature stability have shown that reaction (1) is shifted to lower temperatures under these conditions and occurs already at 1400 °C [3]. The N_2 release and the related mass loss (Fig. 12a) are spread over a long time period of at least 5 h. In contrast to that, reaction (1) proceeds abruptly at 1500 °C (Fig. 12b), indicated by the mass loss and related N_2 release. The N_2 starvation condition at 1500 °C in pure Ar even leads to the formation of silicon in the ZrB_2/Si C N composite (see Fig. 9a). Therefore, the broad N_2 release range is likely to account for the observed ZrC_xN_y formation at 1400 C in Ar. An evaluation of the nitrogen release as a result of the carbothermic reaction (1) gives 0.01 mol of N_2 per Gramm of (liquid) PSZ 20. Therefore, the amount of released nitrogen is sufficient to nitride the whole ZrB_2 that is contained in the ZrB_2/Si C N composite according to the reaction $ZrB_2 + 3/2N_2 = ZrN + 2BN$.

This is in good accordance with experimental work by Brewer et al. [39] (Ti , Zr , W , Cr borides in N_2) and Kiessling et al. [40] (Cr , Fe , W borides in ammonia) who found borides being stable only at the highest temperatures while nitrides are formed at lower temperatures. Brewer et al. found ZrB_2 stable at 1547 °C in 0.5 atm N_2 while modelling (Fig. 4) predicts the reaction $ZrB_2 + 3/2N_2 = ZrN + 2BN$ below 1842 °C under these conditions. This shows that real reaction processes at solid gas interfaces can be determined by their local gaseous environment, such as transport of gaseous educts and products through the gaseous boundary layer, and thus local conditions can be different from global thermodynamic equilibrium.

The progress of the nitriding reaction of ZrB_2 was also confirmed through nitriding of ZrB_2 powder in Ar/N_2 with p_{N2} = 0.5 bar (Fig. 10). The reaction thereby follows linear kinetics at temperatures of 1200 °C, 1300 °C and 1400 °C with an apparent activation energy of about 154 kJ/mol. Due to the limited number of experiments in a limited investigated temperature range this value should be considered as an indicative value lying between nitriding of Si (114 kJ/mol [41]) and Ti (202 kJ/mol [42]) or $TiSi_2$ (245 594 kJ/mol [43]) powders. Deviation from the linear time dependence at 1500 °C must be a result of the superimposition of the nitriding reaction with volatilization effects.

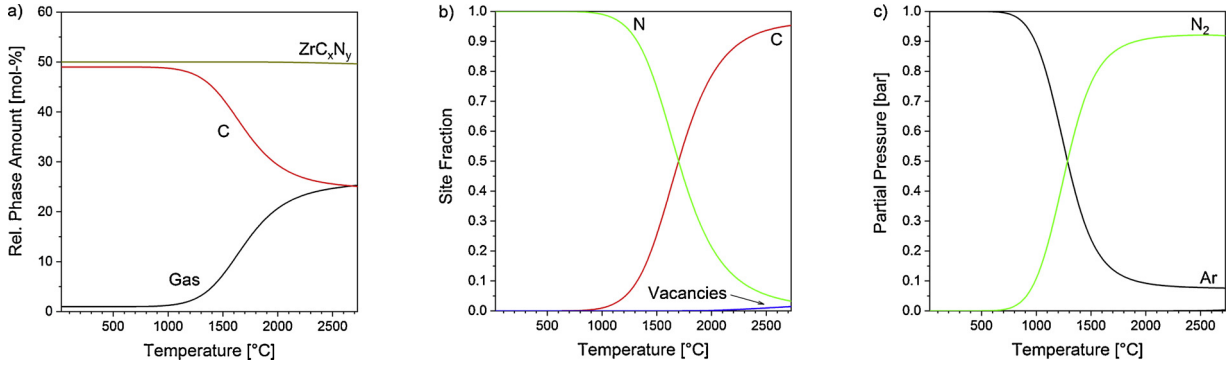

Fig. 6. Calculated a) phase fraction b) site occupancy and c) gas composition for ZrC_xN_y and graphite as a function of temperature.

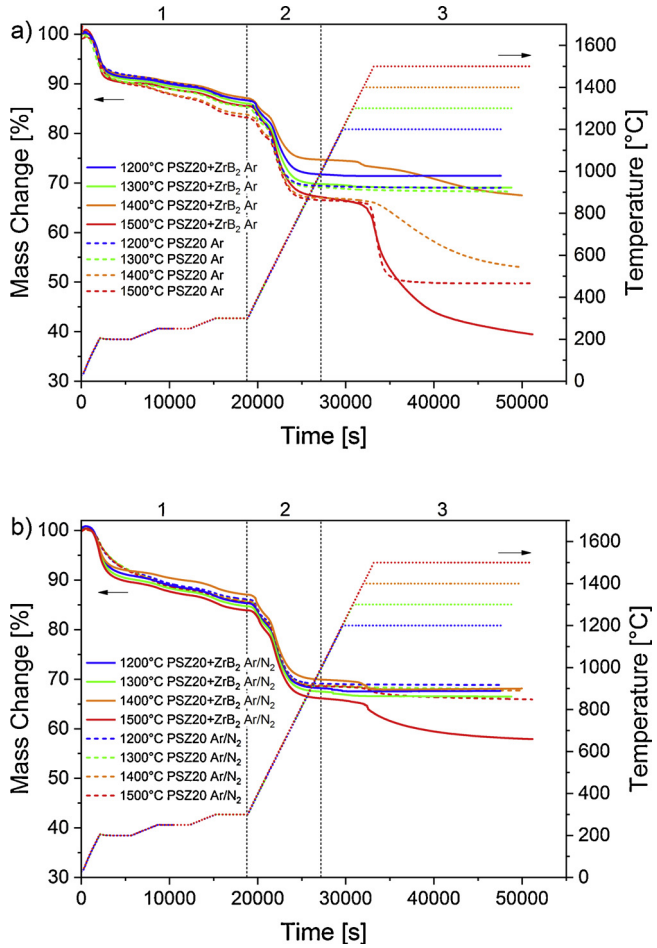

Fig. 7. Thermogravimetric experiments with ZrB_2-filled PSZ 20 in flowing a) Ar and b) Ar/N_2 (p_{N2} = 0.5 bar). Results for pure PSZ 20 [3] are shown for comparison.

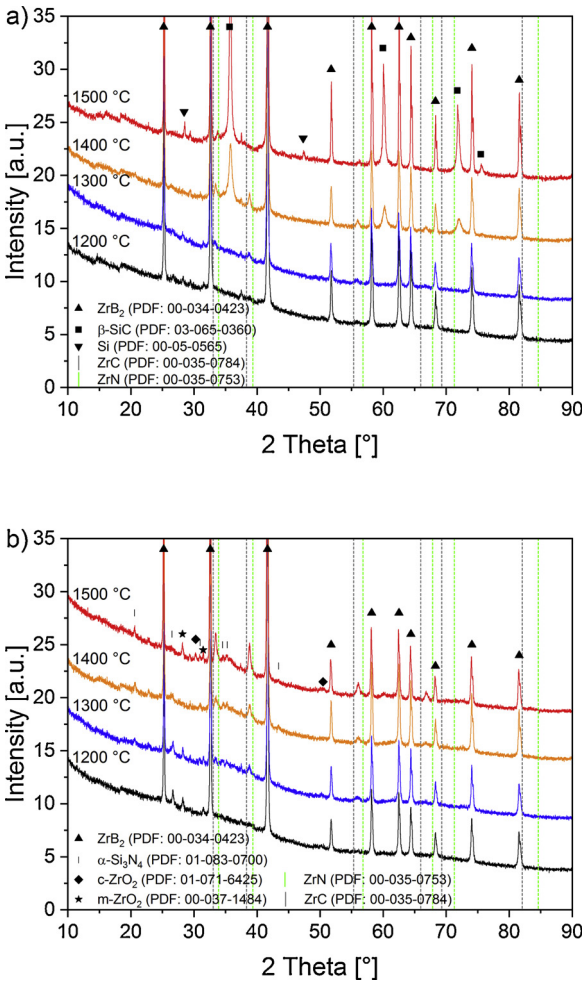

Fig. 9. XRD patterns of ZrB_2/Si-C-N ceramics obtained by pyrolysis in a) Ar and b) in Ar/N_2 up to maximum temperatures of 1200 °C, 1300 °C, 1400 °C and 1500 °C.

This behavior was reproduced in repeated experiments; however, the origin is not clear as no additional phases are found in the XRD analysis (see Fig. 10). Possibly a reaction with the alumina crucible is resulting in the formation of boron oxides which are highly volatile at the highest temperature.

Then ZrC_xN_y is formed by dissolution of C from the Si C N matrix in the ZrN. Due to their same crystal structure and similar lattice constants the system ZrC ZrN exhibits a complete solid solubility [44 47]. Ac cording to work by Bill et al. [35 37] on similar precursor systems, the carbon in the amorphous Si C N ceramic is present in form of CSi_4 as well as mixed SiN_xC_y units (x = 2.3; x + y = 4), and sp^2 hybridized carbon. Therefore, the effective activity of carbon in Si C N is not

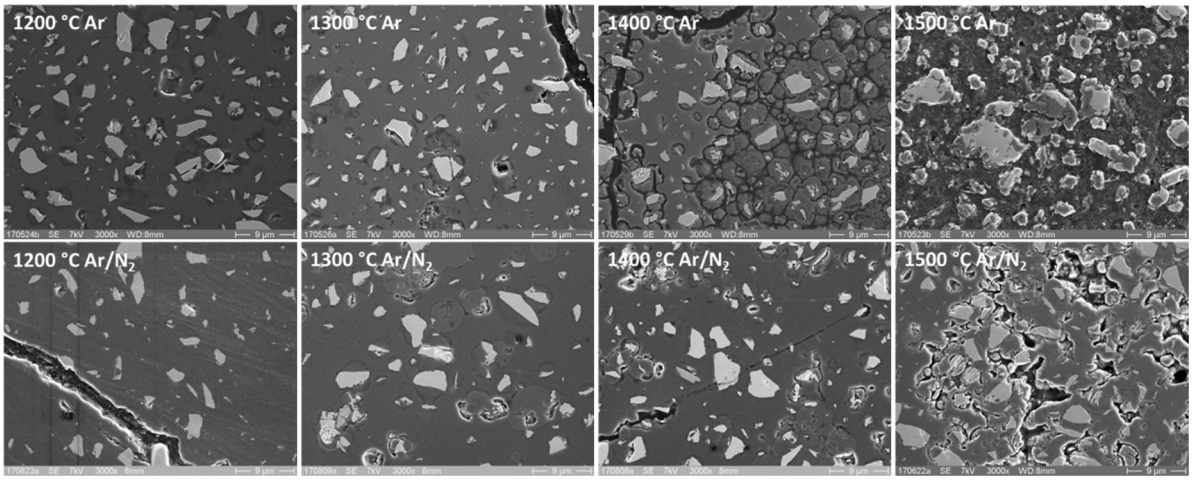

Fig. 8. Microstructure of ZrB_2/Si-C-N ceramics obtained by pyrolysis of ZrB_2-filled PSZ 20 up to maximum temperatures of 1200 °C–1500 °C in flowing Ar and Ar/N_2-atmosphere.

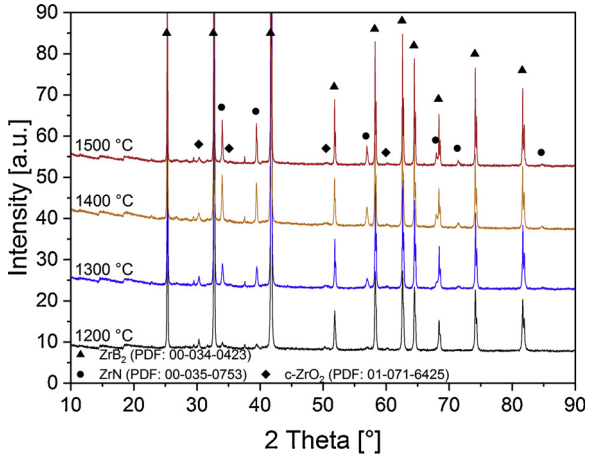

Fig. 10. XRD patterns of ZrB_2-powder annealed for 25 h at 1200 °C, 1300 °C, 1400 °C and 1500 °C in flowing Ar/N_2 (p_{N2} = 0.5 bar).

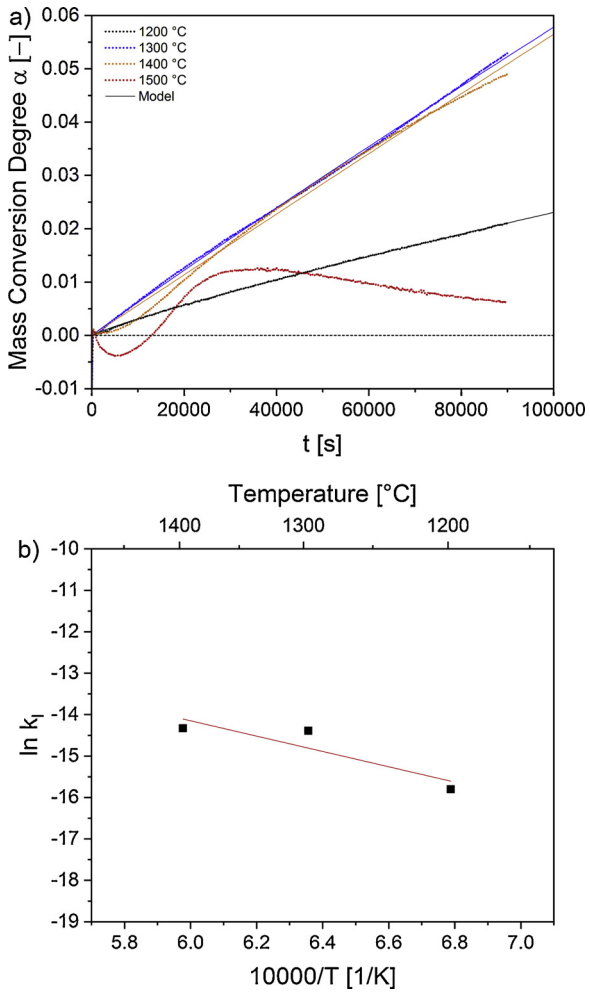

Fig. 11. Obtained a) mass conversion degree α and b) Arrhenius plot of the linear reaction constants of ZrB_2 powder samples.

known. However, Fig. 5 shows the tendency of carbon solubility in ZrC_xN_y as a function of the carbon activity. With decreasing carbon activity, also the carbon content is decreasing. Moreover, the carbon solubility is increasing with the temperature. Fig. 6 shows in addition that the carbon solubility in ZrN is depending on temperature. Below 900 °C ZrN and carbon are chemically inert, coexisting in thermo dynamic equilibrium. For example at 1000 °C ZrC_xN_y with 1 at.% N is

Table 2
Avrami exponent n and linear reaction constant k_l for isothermal nitriding of ZrB_2 powders at p_{N2} = 0.5 bar.

Temperature [°C]	n	k_l	R^2
1200	0.88	$1.37 \cdot 10^{-7}$	0.996
1300	0.98	$5.63 \cdot 10^{-7}$	0.999
1400	1.01	$5.99 \cdot 10^{-7}$	0.994

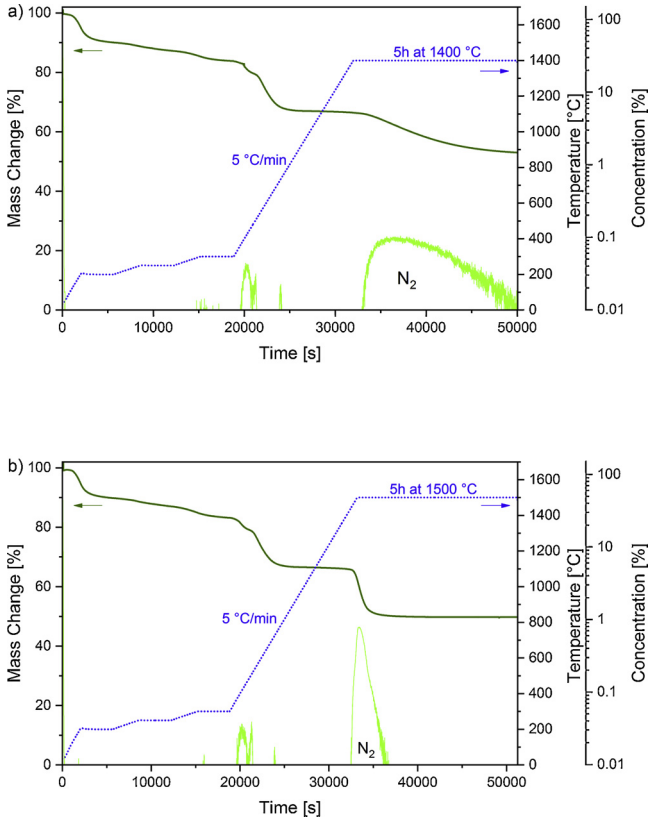

Fig. 12. Thermogravimetric experiment with PSZ 20 heated up to the final pyrolysis temperature of a) 1400 °C and b) 1500 °C in flowing Ar (100 ml/min). The related release of N_2 is indicated [3].

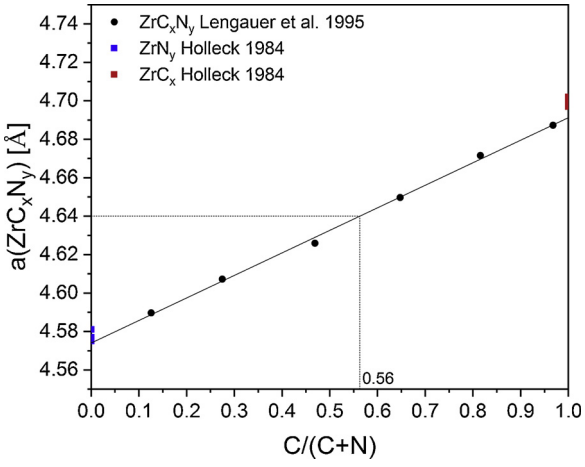

Fig. 13. Lattice parameter of ZrC_xN_y as a function of the composition [49,50]. The measured lattice parameter is indicated.

formed by dissolution of carbon as can be seen from the site occupancy (Fig. 6b) under the release of N_2 (Fig. 6c). This carbon dissolution

increases significantly with higher temperatures (Fig. 13).

The obtained ZrC_xN_y exhibits a lattice parameter of 4.64 Å. As the lattice parameter in the system ZrC ZrN obeys Vegard's law [45,48,49] this corresponds to a carbon fraction of C/(C + N) = 0.56 according to data by Lengauer et al. [49]. In contrast to the composition, a potential sub stoichiometry has a much smaller effect on the lattice parameter [50]. This is in good accordance with work by Sun et al. [18] on a ZrB_2/Si C N composite observing the crystallization of ZrC_xN_y with Zr:C:N = 2:1:1 after annealing above the carbothermic reaction temperature 1500 °C in Ar. However no annealing duration is given.

Sun et al. [18] moreover see a stabilizing effect of ZrB_2 on the carbothermic reaction of the Si C N matrix. We cannot confirm this observation. By normalizing the thermogravimetric experiments during pyrolysis of the ZrB_2/PSZ 20 mixture to the PSZ 20 content we only see a higher scattering compared to pure PSZ 20. Crack formation due to shrinkage during pyrolysis seems to be enhanced as a result of the coefficient of thermal expansion (CTE) mismatch between ZrB_2 (α = 6.6 8.4·10^{-6} K^{-1} [51,52]) and Si C N (α = 3.1 3.5·10^{-6} K^{-1} [53]). According to Aigner et al. [54] the CTE of ZrC_xN_y is in the same range as ZrB_2 (7.8·10^{-6} K^{-1} for C/(C + N) = 0.56). However, the CTE mismatch should be overcome by selecting an appropriate amount and homogeneous distribution of the ZrB_2 particles in the composite.

6. Conclusions

Through targeted application of CALPHAD modelling, the solid state reactions between ZrB_2 particles and the components of the Si C N ceramic matrix were identified. The first reaction to occur upon heating (1597 °C: $ZrB_2 + Si_3N_4 = ZrN + 2BN$ + L(Si,Zr,B,N)) is 113 °C above the application limiting carbothermic reaction temperature (1484 °C: $Si_3N_4 + 3C = 3SiC + 2N_2$) of the Si C N matrix. Therefore, no critical reactions occur in the ZrB_2/Si C N composite, reducing its maximum application temperature compared to the pure Si C N ceramic.

The formation mechanism of ZrC_xN_y was identified combining CALPHAD modelling with key experiments: nitriding of ZrB_2 and pyrolysis of ZrB_2/PSZ 20 mixtures in Ar/N_2 atmosphere. First ZrN is formed from the nitriding reaction of ZrB_2 with the Ar/N_2 atmosphere. Then, as soon as ZrN is present, graphite from the Si C N matrix is solved in ZrN forming the ZrC_xN_y solid solution. Hence ZrC_xN_y formation can be avoided by selection of appropriate pyrolysis conditions during preparation of the ZrB_2/Si C N composite outside the thermodynamic stability range of ZrN, e.g. at low p_{N2} (pure Ar) and moderate temperature below 1400 °C. The potential benefit of the ZrB_2 addition on the high temperature oxidation resistance of the CMC is to be investigated.

Acknowledgements

We gratefully acknowledge the German Federal Ministry of Education and Research (BMBF) for sponsoring this work within the framework of NewAccess (Funding code: 03EK3544A). We also thank Clariant SE, Germany for providing samples of Ceraset® PSZ 20 and ZrB_2 and Dr. H. Leiste for the XRD measurements.

References

[1] H.J. Seifert, J. Peng, H.L. Lukas, F. Aldinger, Phase equilibria and thermal analysis of Si-C-N ceramics, J. Alloys Compd. 320 (2001) 251–261.
[2] H.J. Seifert, H.L. Lukas, F. Aldinger, Development of Si-B-C-N ceramics supported by phase diagrams and thermochemistry, Ber. Bunsenges. Phys. Chem. 102 (1998) 1309–1313.
[3] I.J. Markel, J. Glaser, M. Steinbrück, H.J. Seifert, Experimental and computational analysis of PSZ 10- and PSZ 20-derived Si-C-N ceramics, J. Eur. Ceram. Soc. 39 (2019) 195–204.
[4] P. Greil, Near net shape manufacturing of polymer derived ceramics, J. Eur. Ceram. Soc. 18 (1998) 1905–1914.
[5] P. Greil, Active-filler-controlled pyrolysis of preceramic polymers, J. Am. Ceram. Soc. 78 (1995) 835–848.
[6] G. Stantschev, M. Frieß, R. Kochendörfer, W. Krenkel, Long fibre reinforced ceramics with active fillers and a modified intra-matrix bond based on the LPI process, J. Eur. Ceram. Soc. 25 (2005) 205–209.
[7] J. She, D. Jiang, An attractive way to heal surface defects of some carbide and boride ceramics, Mater. Lett. 26 (1996) 313–317.
[8] B. Kasper, Phasengleichgewichte im System B-C-N-Si, Dissertation Universität Stuttgart (1996).
[9] N.S. Jacobson, G.N. Morscher, D.R. Bryant, R.E. Tressler, High-temperature oxidation of boron nitride: II, boron nitride layers in composites, J. Am. Ceram. Soc. 82 (6) (1999) 1473–1482.
[10] W.G. Fahrenholtz, G.E. Hilmas, Oxidation of ultra-high temperature transition metal diboride ceramics, Int. Mater. Rev. 57 (2012) 61–72.
[11] M.M. Opeka, I.G. Talmy, E.J. Wuchina, J.A. Zaykoski, S.J. Causey, Mechanical, thermal and oxidation properties of refractory hafnium and zirconium compounds, J. Am. Ceram. Soc. 19 (1999) 2405–2414.
[12] F. Liu, J. Kong, C. Luo, F. Ye, X. Luan, N. Tian, Y. Liu, H. Zhang, J. Gu, Y. Tang, High temperature self-healing SiBCN ceramics derived from hyperbranched polyborosilazanes, Adv. Compos. Hybrid. Mater. (2018) 1–12.
[13] A. Müller, P. Gerstel, M. Weinmann, J. Bill, F. Aldinger, Si-B-C-N ceramic precursors derived from dichlorodivinylsilane and chlorotrivinylsilane. 1. Precursor synthesis, Chem. Mater. 14 (8) (2002) 3398–3405.
[14] A. Müller, J. Peng, H.J. Seifert, J. Bill, F. Aldinger, Si-B-C-N ceramic precursors derived from dichlorodivinylsilane and chlorotrivinylsilane. 2. ceramization of polymers and high-temperature behavior of ceramic materials, Chem. Mater. 14 (8) (2002) 3406-2412.
[15] S. Zhu, W.G. Fahrenholtz, G.E. Hilmas, Enhanced densification and mechanical properties of ZrB2–SiC processed by a preceramic polymer coating route, Scripta Mater. 59 (2008) 123–126.
[16] X. Ren, H. Li, Y. Chu, Q. Fu, K. Li, Preparation of oxidation protective ZrB2–SiC coating by in-situ reaction method on SiC-coated carbon/carbon composites, Surf. Coat. Technol. 247 (2014) 61–67.
[17] W. Fahrenholtz, Thermodynamic analysis of ZrB2-SiC oxidation: formation of a SiC-depleted region, J. Am. Ceram. Soc. 90 (2007) 143–148.
[18] Y. Sun, Y. Li, D. Su, S. Wang, Y. Xu, Preparation and charakterization of high temperature SiCN/ZrB2 ceramic composite, Ceram. Int. 41 (2015) 3947–3951.
[19] W.A. Johnson, R.F. Mehl, Reaction kinetics in processes of nucleation and growth, Trans. Am. Inst. Metall. Pet. Eng. 135 (1939) 416–458.
[20] M. Avrami, Granulation, phase change, and microstructure kinetics of phase change. III*, J. Chem. Phys. 9 (1940) 177–184.
[21] A. Kolmogorov, Zur Statistik der Kristallisationsvorgänge in Metallen, Izv. Akad. Nauk SSSR Ser. Mater. 1 (3) (1937) 355–359.
[22] H.L. Lukas, S.G. Fries, B. Sundman, Computational Thermodynamics - The CALPHAD Method, Cambridge University Press, Cambridge, 2007.
[23] Scientific Group Thermodata Europe (SGTE), Grenoble Campus, 1001 Avenue Centrale, BP66, F-38402 Saint Martin d'Heres, France, http://www.sgte.org.
[24] J. Gröbner, H.L. Lukas, F. Aldinger, Thermodynamic calculation of the ternary system Al-Si-C, Calphad 20 (2) (1996) 247–254.
[25] H.M. Chen, F. Zheng, H.S. Liu, L.B. Liu, Z.P. Jin, Thermodynamic assessment of B-Zr and Si-Zr binary systems, J. Alloys Compd. 468 (2009) 209–216.
[26] X. Ma, C. Li, K. Bai, P. Wu, W. Zhang, Thermodynamic assessment of the Zr-N system, J. Alloys Compd. 373 (2004) 194–201.
[27] A.F. Guillermet, Analysis of thermochemical properties and phase stability in the zirconium-carbon system, J. Alloys Compd. 69-89 (2017) 1995.
[28] H.M. Chen, Y. Xiang, S. Wang, F. Zheng, L.B. Liu, Z.P. Jin, Thermodynamic assessment of the C-Si-Zr system, J. Alloys Compd. 474 (2009) 76–80.
[29] H. Duschanek, P. Rogl, MSIT, B-C-Zr Ternary Phase Diagram Evaluation, MSI Materials Science International Services GmbH, 1998.
[30] J.O. Anderson, T. Helander, L. Höglund, P.F. Shi, B. Sundman, Thermo-calc and DICTRA, computational tools for materials science, Calphad 26 (2002) 273–312.
[31] W.M. Guo, L.X. Wu, T. Ma, S.X. Gu, Y. You, H.T. Lin, S.H. Wu, G.J. Zhang, Chemical reactivity of hot-pressed Si3N4–ZrB2 ceramics at 1500–1700°C, J. Eur. Ceram. Soc. 35 (2015) 2973–2979.
[32] W.M. Guo, S.X. Gu, Y. You, Q.G. Jiang, S.H. Wu, H.T. Lin, Densification and thermal stability of hot-pressed Si3N4–ZrB2Ceramics, J. Am. Ceram. Soc. 98 (12) (2015) 3651–3654.
[33] L. Kaufman, Calculation of Multicomponent Refractory Composite Phase Diagrams, MANLABS INC, CAMBRIDGE MA, 1986.
[34] Z. Nasiri, M. Mashhadi, A. Abdollahi, Effect of short carbon fiber addition on pressureless densification and mechanical properties of ZrB2–SiC–Csf nanocomposite, Int. J. Refract. Met. Hard Mater. 51 (2015) 216–223.
[35] J. Bill, T.W. Kamphowe, A. Müller, T. Wichmann, A. Zern, A. Jalowieki, J. Mayer, M. Weinmann, J. Schuhmacher, K. Müller, J. Peng, H.J. Seifert, F. Aldinger, Precursor-derived Si-(B-)C-N ceramics: thermolysis, amorphous state and crystallization, Appl. Organomet. Chem. 15 (2001) 777–793.
[36] J. Bill, J. Schuhmacher, K. Müller, S. Schempp, J. Seitz, J. Dürr, H.P. Lampertner, J. Golczewski, J. Peng, H.J. Seifert, F. Aldinger, Investigations into the structural evolution of amorphous Si-C-N ceramics from precursors, Zeitschrift für Metallkunde 91 (2000) 335–351.
[37] J. Bill, J. Seitz, G. Thurn, J. Dürr, J. Canel, B.Z. Janos, A. Janowiecki, D. Sauter, S. Schempp, H.P. Lamparter, J. Mayer, F. Aldinger, Structure analysis and properties of Si-C-N ceramics derived from polysilazanes, Phys. Status Solidi A 166 (1998) 269–296.
[38] J. Dürr, P. Schempp, P. Lamparter, J. Bill, S. Steeb, F. Aldinger, X-ray and neutron small angle scattering with Si-C-N ceramics using isotopic substitution, Solid State Ionics 101-103 (1997) 1041–1047.
[39] L. Brewer, H. Haraldsen, The thermodynamic stability of refractory borides, J.

Electrochem. Soc. 102 (7) (1955) 399–406.
[40] R. Kiessling, Y.H. Liu, Thermal stability of the chromium, iron, and tungsten borides in streaming ammonia and the existence of a new tungsten nitride, J. Metals 3 (1951) 639–642.
[41] S.W. Yin, L. Wang, L.G. Tong, F.M. Yang, Y.H. Li, Kinetic study on the direct nitridation of silicon powders diluted with α-Si3N4 at normal pressure, Int. J. Min. Metall. Mater. (2013) 493–498.
[42] H. Rode, V. Hlavacek, Detailed kinetics of titanium nitride synthesis, AlChE J. (1995) 377–388.
[43] J. Roger, Maillé, M.A. Dourges, Isothermal nitridation kinetics of TiSi2 powders, J. Solid State Chem. 212 (2014) 134–140.
[44] C. Agte, K. Moers, Methoden zur Reindarstellung hochschmelzender Carbide, Nitride und Boride und Beschreibung einiger ihrer Eigenschaften, Zeitschrift für anorganische und Allgemeine Chemie 198 (1931) 233–275.
[45] H. Bittner, H. Goretzki, F. Benesovsky, H. Nowotny, Über einige Monocarbid-Mononitrid-Systeme und deren magnetische Eigenschaften, Monatshefte für Chemie 94 (1963) 518–526.
[46] R. Kieffer, P. Ettmayer, H. Nowotny, G. Dufek, New investigations concerning miscibility of transition-metal nitrides and carbides, Metall 26 (7) (1972) p. 701.
[47] S. Binder, W. Lengauer, P. Ettmayer, J. Bauer, J. Debuigne, M. Bohn, Phase equilibria in the systems Ti-C-N, Zr-C-N and Hf-C-N, J. Alloys Compd. 217 (1995) 128–136.
[48] K. Constant, R. Kieffer, P. Ettmayer, Über das pseudoternäre System ZrO-ZrN-ZrC, Monatshefte für Chemie 106 (1975) 823–832.
[49] W. Lengauer, S. Binder, K. Aigner, P. Ettmayer, A. Guillou, J. Debuigne, G. Groboth, Solid state properties of group IVb carbonitrides, J. Alloys Compd. 217 (1995) 137–147.
[50] H. Holleck, Binäre und ternäre Carbid- und Nitridsysteme der Übergangsmetalle, Gebrüder Borntraeger, Berlin-Stuttgart, 1984.
[51] N.L. Okamoto, M. Kusakari, K. Tanaka, H. Inui, S. Otani, Temperature dependence of thermal expansion and elastic constants of single crystals of ZrB2 and the suitability of ZrB2 as a substrate for GaN film, J. Appl. Phys. 93 (1) (2003) 88–93.
[52] J.W. Zimmermann, G.E. Hilmas, W.G. Fahrenholtz, Thermophysical properties of ZrB2 and ZrB2-SiC ceramics, J. Am. Ceram. Soc. 91 (5) (2008) 1405–1411.
[53] J. Peng, H.J. Seifert, F. Aldinger, Thermal expansion behavior of precursor-derived amorphous Si-C-N and Si-B-C-N ceramics, J. Mater. Sci. Technol. 18 (2) (2002) 139–142.
[54] K. Aigner, W. Lengauer, D. Rafaja, P. Ettmayer, Lattice parameters and thermal expansion of Ti(CxN1-x), Zr(CxN1-x), Hf(CxN1-x) and TiN1-x from 298 to 1473 K as investigated by high-temperature X-ray diffraction, J. Alloys Compd. 215 (1994) 121–126.